Chapter 4
Laser Shock Peening Effects on Additively Manufactured Ti-6Al-4V

Bryce Parmer, Hunter Blankenship, Dan Fries, and Martha E. Grady

Abstract Additively manufactured (AM) metal parts in aerospace applications started to gain popularity in the 2010s with the mass production of smaller aircraft components using AM metals. AM reduces cost, production time, and increases design freedom compared to traditional methods. However, this manufacturing method creates defects such as porosity and tensile residual stress, so post-processing methods are needed to improve the components. Laser shock peening (LSP) is a recent post-processing method used to induce compressive residual stress to improve the mechanical properties of the component. This study compares wrought Ti-6Al-4V (Ti64) to AM Ti64 that is printed using laser powder bed fusion (L-PBF) in two different orientations (vertically and horizontally). The physical and mechanical properties of Ti64 plates that undergo LSP will be compared. The plate sample properties will be measured using stylus profilometry, atomic force microscopy (AFM), x-ray diffraction (XRD), and scanning electron microscope (SEM). Stylus profilometry and AFM obtain the roughness of the surface, XRD analyzes the near-surface residual stress profile, and SEM optically observes the surface of each of the plates. Four different power densities, 1.74, 3.10, 6.97, and 12.38 GW/cm^2 are explored with the aim to improve the AM Ti64 mechanical and physical properties to be on par with wrought Ti64 or better. Preliminary observations of each of the samples using SEM show that LSP smooths the surface of the plates and melts some of the un-melted particles that were present on the AM Ti64 samples, as expected. However, at the highest power density (12.38 GW/cm^2), some plates showed micro-cracks forming on the peened surface, indicating the existence of an ideal range below this value for net gains in residual stress abatement.

Keywords Laser shock peening · residual stress · AM Ti-6Al-4V · additive manufacturing · laser powder bed fusion

Introduction

Additive manufacturing (AM) as a process of manufacturing metals has been gaining prominence in the aerospace field due to its ability to increase part efficiency, reduce the weight of the part, and its ability to make complex parts as a single component. Though with these advantages, the AM process has the drawback of high cost of manufacturing. The high cost is because AM parts require significant post processing. During the AM process, the part is subject to large thermal gradients that create tensile residual stress. These tensile residual stresses create deformations and lower the fatigue life in the part [1]. One of the most common post-process methods to improve AM metals is hot isostatic pressing (HIP) [2]. HIP has been shown to reduce tensile stresses in the part by 70%, but it cannot fix the cracks that appear during the manufacturing process and not entirely close large and irregular shaped pores [1, 2]. Recent research in the field has been focused on the post-process method of laser shock peening (LSP) to induce compressive residual stress to fix the imperfections that arise during manufacturing [3]. The research here focuses on optimizing the LSP process on AM Ti-6Al-4V (Ti64) by adjusting the laser intensity and number of laser shots to improve properties such as roughness, fatigue life, and residual stresses.

Bryce Parmer · Hunter Blankenship · Dan Fries · Martha E. Grady
Department of Mechanical and Aerospace Engineering, College of Engineering, University of Kentucky, Lexington, Kentucky, USA
e-mail: Bryce.Parmer1@uky.edu; Hunter.Blankenship@uky.edu; dan.fries@uky.edu; m.grady@uky.edu

© The Author(s), under exclusive license to River Publishers 2026

Piyush Thakre et al. (eds.), *Mechanics of Additive and Advanced Manufacturing, Inverse Methods and Machine Learning, Volume 5, 2026*, Conference Proceedings of the Society for Experimental Mechanics Series, https://doi.org/10.13052/rp-9788743815983

Methods and Materials

This research uses a Powerlite 8010 Nd:YAG laser at 1064 nm, 1.20±0.005 J, and a pulse width of 5.45±0.12 ns to induce compressive waves onto AM Ti64 plate samples. Samples were made using an EOS M 290 laser powder bed fusion (LPBF) printer, and were printed into vertical and horizontal 1" x 1" x 0.5" rectangular prisms. The vertical prints were made with the 1" x 0.5" face on the baseplate and the horizontal prints were made with the 1" x 1" face on the baseplate. These were then cut using a wire-EDM into 1" x 1" plates with a thickness of 1.3 mm to be used on the optics table for LSP. For comparison, wrought Ti64 was cut into the same dimensions and underwent the same tests. The optics table layout utilized a biconvex lens and motorized stages as shown in Figure 1. Using these, the LSP process was done at 4 different power densities that were controlled by changing the spot size of the laser. Spot sizes were 4 mm (1.74 GW/cm^2), 3 mm (3.10 GW/cm^2), 2 mm (6.97 GW/cm^2), and 1.5 mm (12.38 GW/cm^2). These values were calculated using Eq. (1) (with Eq. (2) using values for the 4 mm spot size case) [4], where E is the measured energy of the laser, A is the spot size, and τ is the pulse width. The motorized stages were programmed to move such that the plates had 0% overlap on the shots and 50% overlap on the shots to compare single and double shots.

$$S = \frac{E}{A\tau} \tag{1}$$

$$S = \frac{1.2\ [J]}{(\pi * (4/2)^2\ [mm^2]) * 5.483\ [ns]} = 1.74\ \left[\frac{GW}{cm^2}\right] \tag{2}$$

After LSP, each of the plate samples were imaged using a FEI Quanta E-SEM, a scanning electron microscopy (SEM) machine, in the peened and unpeened areas. Before imaging, all of the samples were cleaned using acetone, then methanol to wipe down the plates. Then, an air compressor was used to remove contaminants on the sample. Some of the SEM images taken are shown in Figure 2; all four of them are representative images of the vertically printed AM Ti64 at each spot size and its corresponding power density.

After imaging, a stylus profilometer (Bruker Dektak XT Surface Profiler) was used to scan the surface profiles of the peened and unpeened areas. Each sample had two surface profiles obtained in the peened and unpeened areas. All of the sample lengths were 1 mm and the stylus used was a 2 μm radius. Both the images and graphs are used for qualitative comparisons of the LSP process shown in Figure 3. For a more quantitative comparison, the surface roughness was calculated using the root mean square method shown in Eq. (3) [5]. In the equation, L is the test length of 1 mm and z is the measured height measured in the surface profile. Table 1 is the tabulated data of roughness values of a AM Ti64 and wrought Ti64 sample before and after LSP.

$$R_q = \left(\frac{1}{L}\int z^2 dz\right)^{\frac{1}{2}} \tag{3}$$

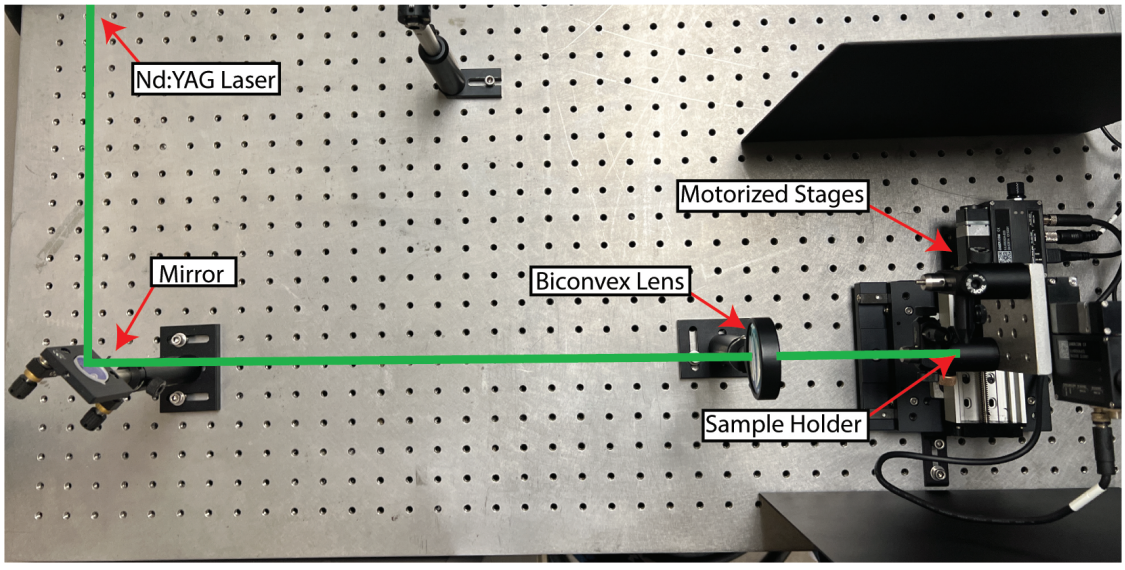

Fig. 1 Optics table layout for LSP.

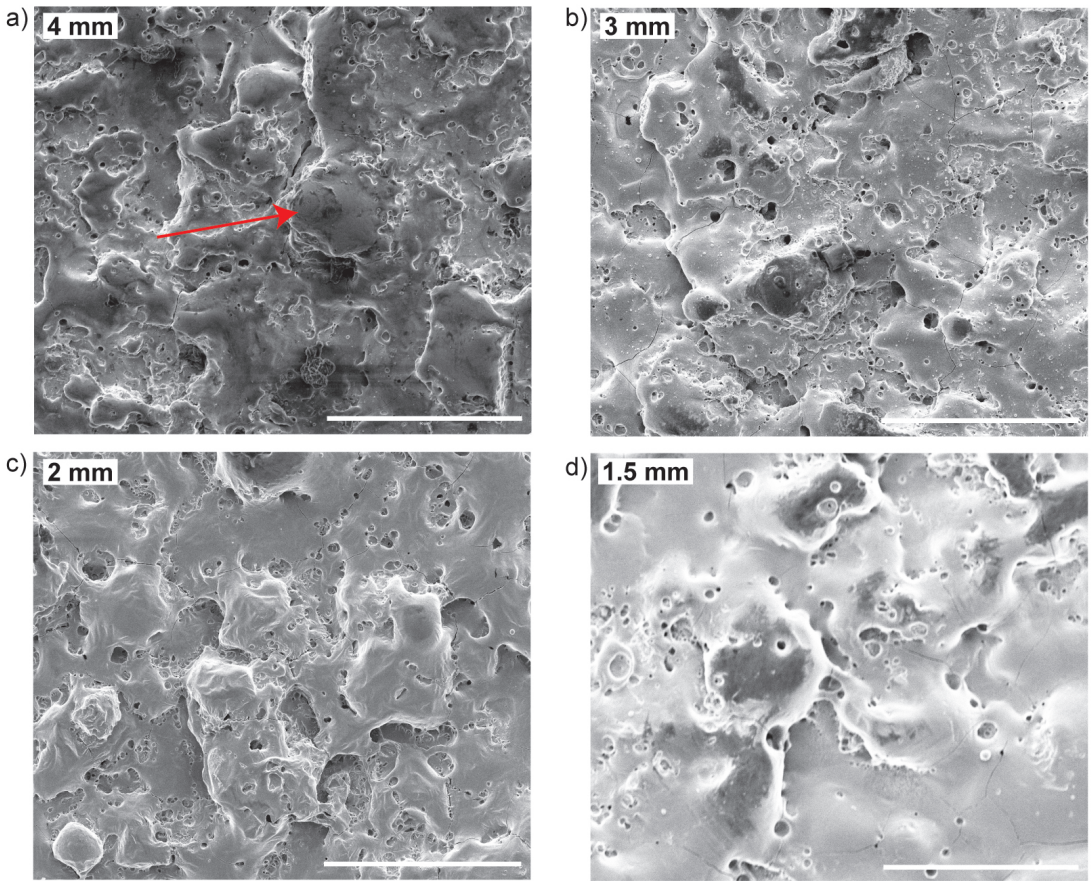

Fig. 2 SEM images of vertically printed AM Ti64 plates subjected to LSP at single shot with varying spot sizes (4, 3, 2, and 1.5 mm). The red arrow in 2a points to an unmelted AM Ti64 particle. Images are at x1000 magnification and all scalebars are 50 μm.

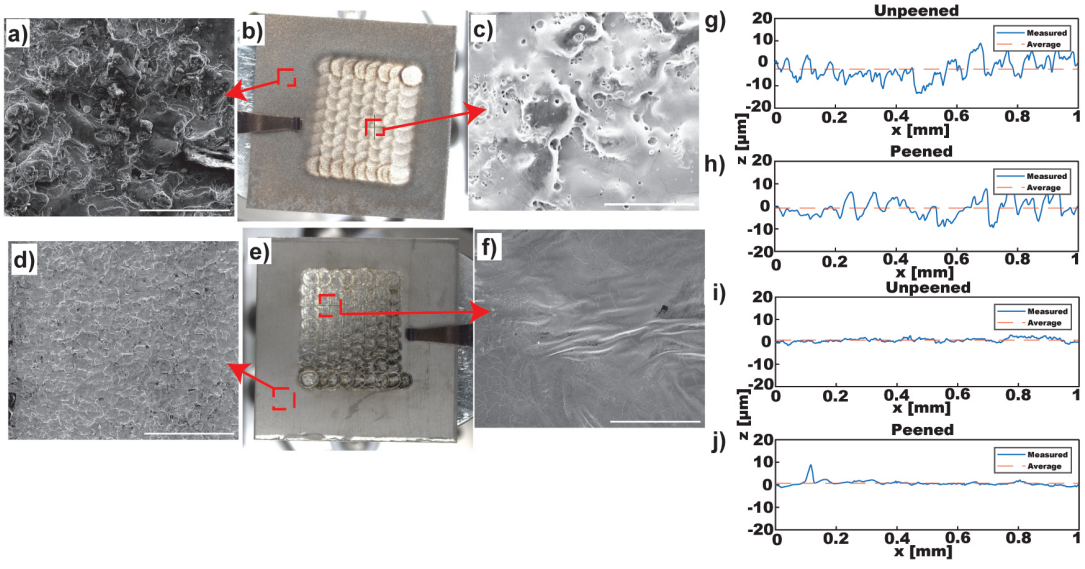

Fig. 3 Data from samples before and after subjected to LSP at a spot size of 1.5 mm a) SEM of vertically printed AM Ti64 sample, b) SEM of wrought Ti64 sample, c) surface profiles of sample shown in a) for peened and unpeened area, d) surface profiles of sample shown in b) for peened and unpeened area. All scalebars are 50 μm and magnification of SEM is at x1000.

Table 1 Wrought and AM Ti64 samples surface roughness before and after LSP at a 1.5 mm spot size and single shot.

Sample Type	Subjected to LSP	Rq (μm)
Wrought Ti64	LSP	1.353 ± 0.2642
	No LSP	0.4056 ± 0.2863
Vertically printed AM Ti64	LSP	4.2834 ± 0.3328
	No LSP	5.1878 ± 0.9602

Preliminary Results

After the LSP process at the various power densities and number of shots, the samples were taken to the SEM for a qualitative, visual analysis shown in Figures 2, 3a, and 3b. Images were taken of the peened and unpeened areas. After SEM imaging, the samples were then taken to the stylus profilometer to get the surface profiles shown in Figures 3c and 3d. The surface profiles were then used to calculate the root mean square roughness and recorded in Table 1.

Discussions and Conclusions

Looking at the images in Figure 2, there is a clear improvement in the surface of the AM Ti64 as the power density of the laser increases (decreasing spot size). The images in Figure 2a show that there is still a largely uneven and rough surface. While the larger un-melted particles that were present on the surface were re-melted to smooth the surface, the power density used was not enough to fully melt them down to the rest of the surface. This is shown in the middle of Figure 2a, located by the red arrow, where the outline of the particle is still present in the circular rise in the surface and is in the range of unmelted Ti64 particles used in LSP, 15-45 μm [6]. Small crevasses and holes from the manufacturing process were not filled. From the qualitative data shown in Figure 2a, it can be inferred that the compressive force induced by LSP was not strong enough by itself to fix the topological imperfections from the manufacturing process.

When comparing images in Figure 2a to 2d, there is a clear improvement seen. The surface on Figure 2d is more flat, with significantly less crevasses and holes, meaning that the LSP process at a power density of 12.38 GW/cm^2 is more effective than at 1.74 GW/cm^2. The smoother surface and decrease in unmelted particles is not without some drawbacks as microcracks can be seen in Figure 2d. While the induced compressive stresses could better smooth the surface of the sample, they began to form microcracks along the surface of the plate. This is also shown in Figure 3, where Figure 3a is the surface profile of the sample shown in Figure 2d. In Figure 3a, the peened surface is smoother shown by the smaller Rq value in table 1 when compared to the as-built area. The peened graph in Figure 3c also displays smoother features. The small, jagged sections between the peaks and valleys present in the unpeened graph are not as prominent in the peened one. The presence of the large peaks and valleys still in the peened graph can be seen visually in Figure 3a, where there are still rough features and crevasses present on the surface. When comparing this sample to a wrought Ti64 sample shown in Figure 3b, signs of warping and microcracks appear on the surface profile of the wrought plate, causing the jumps at the test lengths at 0.12 mm and 0.5 mm on the peened graph. When looking at the roughness values in Table 1, the values are more than triple after LSP for the wrought samples while they decrease by 0.9044 μm for the AM sample. Using these preliminary results, the results of LSP can be seen to improve AM Ti64 as shown qualitatively in the SEM images, surface profiles, and their roughness values. For applications in the aerospace industry, LSP and HIP can both be used on AM Ti64 samples as a way to improve the properties of the metal that were not fully perfected after just HIP.

Future Directions

Future steps of the research will focus on the mechanical properties of the samples and how LSP has changed them. The topical residual stress will be gathered using the data obtained from x-ray diffraction (XRD) measurements. As mentioned previously, tensile residual stress is a large issue in AM metals during the manufacturing process so this will allow for the improvements of fatigue life of AM Ti64 to be quantified by showing the changes from tensile to compressive residual stress. The data will also be compared to the previously gathered qualitative data of the SEM images and surface profiles to see if they matched the conclusions made with them.

Acknowledgments This material is based upon work supported by the National Science Foundation CAREER Award Grant No. 2045853. Any opinions, findings, and conclusions or recommendations expressed in this material are those of the author(s) and do not necessarily reflect the views of the National Science Foundation. We gratefully acknowledge support by the Lighthouse Beacon Foundation for completion of these experiments.

References

1. Kalentics, N., de Seijas, M. O. V., Griffiths, S., Leinenbach, C., & Logé, R. E. (2020). 3D laser shock peening – A new method for improving fatigue properties of selective laser melted parts. Additive Manufacturing, 33, 101112. https://doi.org/https://doi.org/10.1016/j.addma.2020.101112
2. Poulin, J. R., Kreitcberg, A., & Brailovski, V. (2021). Effect of hot isostatic pressing of laser powder bed fused Inconel 625 with purposely induced defects on the residual porosity and fatigue crack propagation behavior. Additive Manufacturing, 47, 102324. https://doi.org/https://doi.org/10.1016/j.addma.2021.102324
3. Dilshad Alam Digonta, H. M., & Fatemi, A. (2024). Laser shock peening and its effects and modeling on fatigue performance of additive manufactured metallic materials. Theoretical and Applied Fracture Mechanics, 130, 104281. https://doi.org/https://doi.org/10.1016/j.tafmec.2024.104281
4. MIT OpenCourseWare. (n.d.). Online textbook: Classical mechanics: Physics. MIT OpenCourseWare. https://ocw.mit.edu/courses/8-01sc-classical-mechanics-fall-2016/pages/online-textbook/
5. Thomas, T. R. (1981). Characterization of surface roughness. Precision Engineering, 3(2), 97-104. https://doi.org/https://doi.org/10.1016/0141-6359(81)90043-X
6. Fousová, M., Vojtěch, D., Kubásek, J. í., Jablonská, E., & Fojt, J. (2017). Promising characteristics of gradient porosity Ti-6Al-4V alloy prepared by SLM process. Journal of the Mechanical Behavior of Biomedical Materials, 69, 368-376. https://doi.org/https://doi.org/10.1016/j.jmbbm.2017.01.043